Macromolecules

Article

pubs.acs.org/Macromolecules

# Thiophene-Based Microporous Polymer Networks via Chemical or Electrochemical Oxidative Coupling

Alex Palma-Cando,[†] Gunther Brunklaus,[‡] and Ullrich Scherf*[,†]

[†]Macromolecular Chemistry Group, Bergische Universität Wuppertal, Gaußstraße 20, D-42119 Wuppertal, Germany

[‡]Institut für Physikalische Chemie, Westfälische Wilhelms-Universität, Corrensstr. 46, D-48149 Münster, Germany

Supporting Information

**ABSTRACT:** Four thiophene-based monomers have been synthesized by Stille- or Suzuki-type couplings followed by chemical or electrochemical polymerization into microporous polymer networks (MPNs) with high BET surface areas ($S_{BET}$). Similar $S_{BET}$ values of up to 2020 and 2135 $m^2\ g^{-1}$ have been determined for tetraphenylmethane-cored bulk MPN powders and thin films, respectively. Electrochemical polymerization in boron trifluoride diethyl etherate (BFEE)/dichloromethane (DCM) mixtures allows for the generation of MPN films with optimized porosity. Moreover, an interesting effect of boron trifluoride on the connectivity of the monomeric units during electropolymerization is observed for 3-thienyl-based monomers. Finally, the electrochemical reduction of 1,3,5-trinitrobenzene at MPN-modified glassy carbon (GC) electrodes shows increased cathodic responses compared to nonmodified GC electrodes due to interaction between electron-deficient nitroaromatic analyte and electron-rich MPN film. The influence of the specific surface area of MPNs on the electrochemical response is also studied for this class of materials.

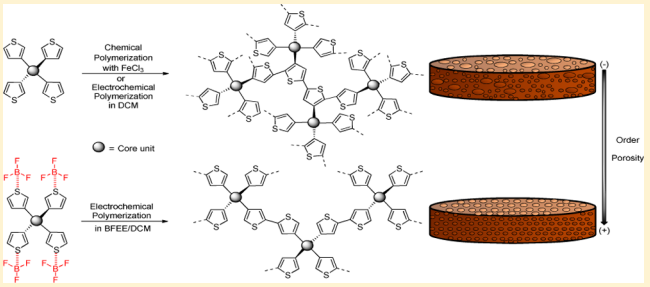


## INTRODUCTION

Microporous polymer networks (MPNs) have attracted enormous attention in the materials science community due to their promising properties: high surface area, well-distributed porosity, chemical and thermal resistance, possible incorporation of various functional groups, among others. Hence, MPNs promise a high application potential in gas capture and separation,[1−6] catalysis,[7−11] organic electronic devices,[12−14] and sensors.[15−17] Up to now, the highest BET surface area ($S_{BET}$) for a MPN material (6461 $m^2\ g^{-1}$) was reported by Zhou et al.[18] for a network composed of interconnected tetraphenylsilane cores. However, synthesis of MPNs with surface areas of >2000 $m^2\ g^{-1}$ is still a challenge.[19] Thiophene-based MPNs are especially interesting due to their possible applications in electronic devices and for gas storage. Yu et al.[20] reported thiophene-based MPNs for $H_2$ storage with $S_{BET}$ of 971 $m^2\ g^{-1}$ and $H_2$ uptake of 3.6 wt % at 77 K. Thomas et al.[21] synthesized thienylene−arylene networks with $S_{BET}$ of 1060 $m^2\ g^{-1}$. Nevertheless, these materials have been obtained as insoluble powders. Processing MPNs into thin films or layers is a major challenge toward many practical applications. A way to overcome the processing problems is an electrochemical polymerization of multifunctional monomers on a suited substrate. Until now, mostly carbazole-based monomers have been electropolymerized due to their low oxidation potential. Ma et al. reported carbazole-based MPNs for use as charge injecting/extracting interlayers in OLEDs,[22] OPV devices,[23] and supercapacitors.[24] Jiang et al. reported MPN-based thin films with high $S_{BET}$ values of up to 2190 $m^2\ g^{-1}$ (determined by Kr adsorption/desorption) for application in sensors[25,26] or for the creation of energy transfer cascades.[27] We have recently reported a direct relation between the number of carbazole moieties in the monomer and the obtained $S_{BET}$ of electrogenerated MPN films as well as the use of the MPN films as electrochemical sensors for nitroaromatic analytes.[28] On the other hand, the electrochemical polymerization of multifunctional thiophene monomers was first reported by Roncali et al.[29] The obtained 3D structures can show an increased electrical conductivity as demonstrated by Müllen and Heinze[30] comparing 3D networks with weakly interacting aggregates of isolated terthiophene-substituted phenylene dendrimers. Thomas et al.[31] recently synthesized dithienothiophene-based microporous polymer films with interesting electrochromic properties by electropolymerization. In the electropolymerization of thiophene-based monomers, it has been shown that the necessary polymerization potential can be strongly reduced by adding boron trifluoride diethyl etherate (BFEE) due to interactions between thiophene rings and boron trifluoride.[32−35] Moreover, the mechanical and electrical properties of the resulting films were improved by using BFEE as additive.

In this study, we synthesized four tetrathienyl-substituted rigid monomers in Stille- or Suzuki-type coupling reactions. Microporous polymer networks were obtained as powders by oxidative polymerization of the monomers with iron trichloride

**Received:** August 17, 2015
**Revised:** September 14, 2015
**Published:** September 18, 2015

  

DOI: 10.1021/acs.macromol.5b01821
*Macromolecules* 2015, 48, 6816−6824

showing specific surface areas ($S_{BET}$) of up to 2020 $m^2\ g^{-1}$ from nitrogen gas sorption measurements. Optical and thermal properties as well as the gas sorption behavior are provided for these bulk MPNs. Correspondingly, electrochemically generated MPN films have been produced in boron trifluoride/dichloromethane mixtures showing $S_{BET}$ values of up to 2135 $m^2\ g^{-1}$ (calculated from krypton gas adsorption/desorption). The MPN films produced in the presence of boron trifluoride exhibited higher specific surface areas and a more defined electrochemical behavior if compared to the corresponding networks made in the absence of boron trifluoride probably due to the exclusive formation of bithiophene connections. The thin films of our MPNs show a rather low surface roughness of only 3−5 nm for film thicknesses of 30−50 nm. Electrochemical reduction of 1,3,5-trinitrobenzene at glassy carbon electrodes modified with our thiophene-based MPNs clearly indicates a direct relationship between specific surface area and current response via an adsorption-controlled interaction of the electron-poor nitroaromatic compound and the electron-rich thiophene-based MPN.

## EXPERIMENTAL SECTION

**Synthesis.** Synthetic details for 2,2′,7,7′-tetra(thien-2-yl)-9,9′-spirobifluorene (SpTh), 2,2′,7,7′-tetra(thien-3-yl)-9,9′-spirobifluorene (Sp3Th), tetra[4-(thien-2-yl)phenyl]methane (TPTTh), and tetra[4-(thien-3-yl)phenyl]methane (TPT3Th) as well as the $FeCl_3$-mediated syntheses of the corresponding bulk polymer networks are reported in the Supporting Information. Solution $^1H$ and $^{13}C$ NMR spectra were obtained on Bruker Avance III 600 machine. APLI mass spectra were recorded on a Bruker Daltronik microTOF system (KrF*-Laser ATLEX-SI, ATL Wermelskirchen). Elemental analyses were carried out on a PerkinElmer 240 B. Thermogravimetric analyses were recorded under argon flow on a Mettler Toledo TGA/DSC1 STAR system. Solid state $^{13}C\{^1H\}$ cross-polarization magic-angle spinning (CPMAS) spectra were measured at 50.33 MHz using a Bruker AVANCE III 200 NMR spectrometer. FT-IR and UV−vis spectra were recorded on a JASCO FT/IR-4200 and V-670, respectively, and photoluminescence spectra on a HORIBA Scientific FluoroMax-4 spectrofluorometer. Nitrogen and krypton adsorption−desorption isotherms were recorded on a BEL Japan Inc. Belsorp-max system at 77 K. All samples were dried on a Belprep-vac II at 140 °C and ∼2 Pa overnight prior to the sorption measurements. AFM images were recorded on an atomic force microscope (Bruker diInnova) operated in tapping mode. The average surface roughness was extracted from the topography images. The thickness of the films was measured with a surface profilometer (Vecco Dektak 150).

**Electropolymerization of Thiophene-Based Monomers and Electrochemical Reduction of 1,3,5-Trinitrobenzene.** Dichloromethane (HPLC grade) was refluxed over phosphorus pentoxide for 3 h and distilled. For electrochemical polymerization and characterization a potentiostat/galvanostat PAR VersaSTAT 4 was used in combination with a three-electrode cell. 10 mL of 0.1 mM solutions of the monomers was prepared in dichloromethane (DCM) or BFEE/DCM (1:4) using 0.1 M $TBABF_4$ as supporting electrolyte. The solutions were placed in a three-electrode cell under an argon atmosphere at 25 °C. A platinum disk electrode (Pt, 1 mm diameter), ITO on glass (∼1.5 × 1.2 cm deposit area), or a glassy carbon disk electrode (GC, 1 mm diameter) was used as a working electrode (WE), platinum as counter electrode (CE), and $Ag°/AgNO_3$ (0.01 M $AgNO_3$/0.1 M TBAP in acetonitrile; 0.53 V vs NHE, nonaqueous reference) or $Ag°/AgCl_{(sat.)}$ (NaCl 3 M, 0.21 V vs NHE, aqueous reference) as a reference electrode (RE). Potentiodynamic or potentiostatic regimes were applied for the deposition of microporous films on the electrodes. Thin MPN films on Pt and ITO were obtained in a dynamic regime by applying multiple cycles from 0 to 1.2 V (SpTh, Sp3Th, TPTTh) or 0−1.3 V (TPT3Th) with a scan rate of 0.10 $V\ s^{-1}$. Thick films on ITO were produced by applying a static oxidative potential of 1.2 V (SpTh, Sp3Th, TPTTh) or 1.3 V (TPT3Th) for 20 min. A potential of 0 V was applied for 60 s in order to discharge (dedoped) the deposits. After removal from the electrodes, rinsing, and careful drying, these films can be used for krypton gas sorption measurements. PTPTTh-modified GC electrodes were produced by applying a potential of 1.2 V until the required polymerization charge (0.01−0.50 mC) was accumulated. After polymerization, a potential of 0 V was applied for 30 s in order to discharge the deposits. PTPTTh-modified GC electrodes were rinsed and used as WE in aqueous 0.2 M KCl and 0.1 M PBS (pH 7.4, Ar atmosphere) at 25 °C. For electrochemical reduction of 1,3,5-trinitrobenzene (TNB) linear scan voltammograms were recorded from 0 to −1 V with a scan rate of 0.01 $V\ s^{-1}$. Aliquots of TNB from stock solutions in acetonitrile were added to the buffered aqueous solution by adjusting the concentration of the nitroaromatic analyte from 0 to 3.0 $\mu$M.

## RESULTS AND DISCUSSION

Synthesis of tetrasubstituted thiophene-based monomers was carried out following literature procedures (see the Supporting Information for details). Scheme 1 shows the chemical structures of the series of thiophene-based monomers studied. 2,2′,7,7′-Tetra(thien-2-yl)-9,9′-spirobifluorene (SpTh) and tetra[4-(thien-2-yl)phenyl]methane (TPTTh) were obtained by Stille-type coupling between 2,2′,7,7′-tetrabromo-9,9′-spirobifluorene or tetra(4-bromophenyl)methane with tributyl(thien-2-yl)stannane. The corresponding 2,2′,7,7′-tetra(thien-3-yl)-9,9′-spirobifluorene (Sp3Th) and tetra[4-(thien-3-yl)-phenyl]methane (TPT3Th) monomers were synthesized by Suzuki-type coupling with thien-3-ylboronic acid.

**Scheme 1. Chemical Structures of the Investigated Thiophene-Based Monomers: (a) SpTh, (b) Sp3Th, (c) TPTTh, and (d) TPT3Th**

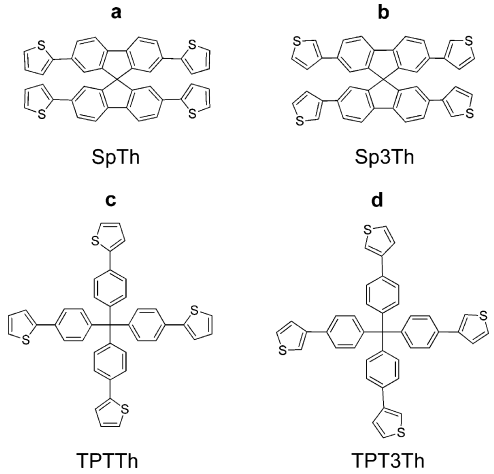


Oxidative chemical polymerization of the four monomers was carried out with iron trichloride in chloroform at room temperature to produce microporous polymers networks (MPNs) in high yields. Thermogravimetric analysis of all MPNs showed good stability up to 450 °C under argon (Figure S1). Solid-state $^{13}C\{^1H\}$ cross-polarization magic-angle spinning (CPMAS) spectra of the MPNs are depicted in Figure 1. All spectra well agree with the proposed chemical structures (insets). Peaks at ca. 65 ppm are attributed to the tetrasubstituted aliphatic carbons. Signals from 115 to 135 nm were related to protonated benzene and thiophene carbons, while signals at low field from 135 to 155 nm reflect nonprotonated aromatic carbons. Absorption (diffuse reflec-



DOI: 10.1021/acs.macromol.5b01821
Macromolecules 2015, 48, 6816−6824

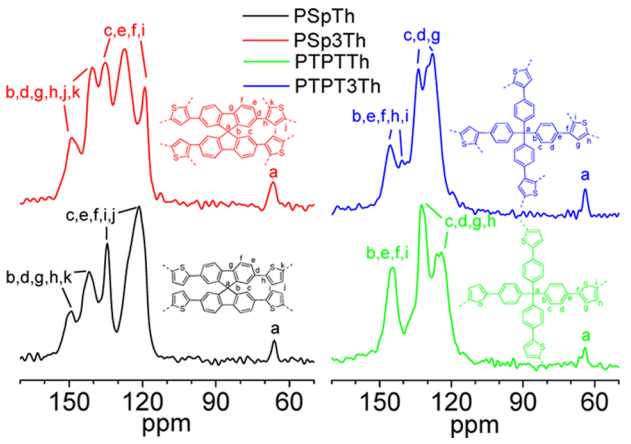


**Figure 1.** $^{13}C\{^1H\}$ CPMAS NMR spectra of bulk polymers networks.

tion) and photoluminescence (PL) spectra are shown in Figure S2. The bulk polymers show broad PL bands with peak maxima at 524 nm (PTPTTh), 547 nm (PSpTh), 581 nm (PSp3Th), and 616 nm (PTPT3Th).

The specific surface area of porous materials is usually determined by applying the Brunauer–Emmett–Teller (BET) equation to gas sorption isotherms at different temperatures.[36−38] Figure 2 shows nitrogen adsorption/desorption

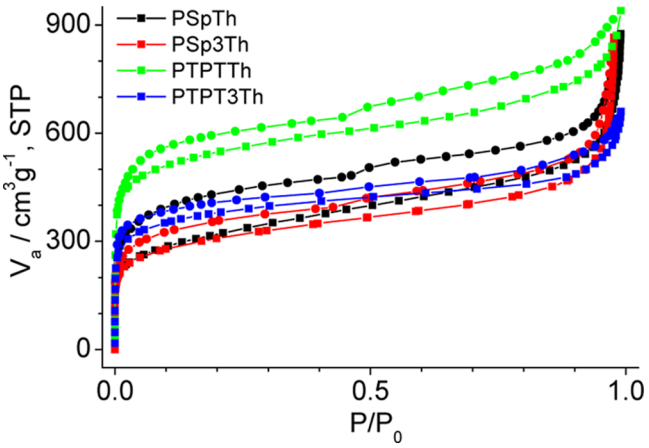


**Figure 2.** Nitrogen gas sorption isotherms of chemically synthesized MPN bulk polymers (oxidation with $FeCl_3$).

isotherms for all bulk polymers. A combination of type I and II isotherms, according to the IUPAC,[39] is observed for the MPNs as typical signature of microporous materials. Fast increase of volume of sorbate at relatively high pressure (>0.9) is assigned to interparticular porosity (meso- and macropores).[40] The specific surface areas were calculated by the BET equation ($S_{BET}$) and are listed in Table 1. A remarkably high $S_{BET}$ of 2020 $m^2\ g^{-1}$, to the best of our knowledge the highest for thiophene-based MPNs, was obtained for PTPTTh which might be related to the presence of a largely continuous porous network. The latter assumption is supported by comparing $S_{BET}$ values of the two MPNs made from 2-thienyl-substituted monomers that can only form bithiophene bridges in the oxidative coupling (SpTh and TPTTh in Scheme 1), with the values for the two MPNs made from 3-thienyl-substituted monomers that are able to form multiple linkages in 2- and 5-positions of the thiophene rings (Sp3Th and TPT3Th in Scheme 1). For both core units, the $S_{BET}$ values for the condensation products of the 2-thienyl-subtituted monomers, PSpTh (1153 $m^2\ g^{-1}$) and PTPTTh (2020 $m^2\ g^{-1}$), are higher compared to PSp3Th (1102 $m^2\ g^{-1}$) and PTPT3Th (1390 $m^2\ g^{-1}$) made from 3-thienyl-substituted monomers. The effect is much more pronounced for tetraphenylmethane-cored MPNs (PTPTTh and PTPT3Th); moreover, their specific surface areas are generally higher as those of the corresponding spirobifluorene-cored MPNs (PSpTh and PSp3Th). The tetraphenylmethane-cored MPNs are characterized by a high structural symmetry, which may cause a more regular porosity and increased specific surface area of the MPNs.

MPNs possessing high specific surface areas might find applications in gas storage and separation (see Figure S3). The pore volumes of our materials are in the range of 0.82−1.22 $cm^3\ g^{-1}$ (see Table 1). Generally, higher gas uptakes for $H_2$, $N_2$, $CH_4$, and $CO_2$ are obtained for the tetraphenylmethane-cored MPNs. This difference can be partially related to different pore sizes of the materials which have been calculated from a nonlocal density functional theory (NLDFT) model resulting in pore diameters of ca. 1.43 nm for the tetraphenylmethane-cored MPNs and reduced pore diameters of ca. 0.40 nm for the spirobifluorene-cored MPNs. The selectivities of gas adsorption by applying Henry's law for $CO_2/N_2$ and $CO_2/CH_4$ at 298 K were 12.1 and 2.8 (SpTh), 11.5 and 2.6 (Sp3Th), 6.6 and 2.4 (PTPTTh), and 10.5 and 2.6 (PTPT3Th), respectively. Strikingly, the increased $S_{BET}$ value of PTPTTh (2020 $m^2\ g^{-1}$) leads to a reduced $CO_2/N_2$ selectivity (6.6) that is caused by an increased nitrogen uptake.

Electrochemical, oxidative polymerization is a proper technique for producing uniform thin films of MPNs on various electrodes in monomer/electrolyte mixtures.[42,43] Several advantages over chemical polymerization exist, among others, a metal- and catalyst-free reaction, short reaction times, simultaneous film formation and deposition, simple doping and dedoping, and the possibility of *in situ* characterization. Electrochemical polymerization of mostly bifunctional thiophene monomers into linear polymers was extensively reported in relation to potential applications in the field of organic electronics (especially electrochromic devices).[44−47] Only a few examples for the electrosynthesis of three-dimensional, conjugated polymer networks have been reported, e.g., based

**Table 1. Porosity Data, Gas Uptake (at 298 K), and Selectivity of Chemically Synthesized Bulk MPNs**

| | | | gas uptake [%] | | | | selectivity[c] | |
|---|---|---|---|---|---|---|---|---|
| polymer | $S_{BET}$ [$m^2\ g^{-1}$] | pore vol[a] [$cm^3\ g^{-1}$] | $CO_2$ | $N_2$ | $CH_4$ | $H_2$[b] | $CO_2/N_2$ | $CO_2/CH_4$ |
| PSpTh | 1153 | 0.90 | 7.19 | 0.38 | 0.92 | 1.38 | 12.1 | 2.8 |
| PSp3Th | 1102 | 0.85 | 6.88 | 0.38 | 0.95 | 1.37 | 11.5 | 2.6 |
| PTPTh | 2020 | 1.22 | 7.61 | 0.73 | 1.15 | 1.81 | 6.6 | 2.4 |
| PTPT3Th | 1390 | 0.82 | 7.88 | 0.48 | 1.10 | 1.67 | 10.5 | 2.6 |

[a]Determined at $P/P_0$ = 0.95. [b]Measured at 77 K. [c]Calculated by applying Henry's law.[15,41]



DOI: 10.1021/acs.macromol.5b01821
*Macromolecules* 2015, 48, 6816−6824

on twisted bithiophene monomers with four 3,4-ethylenedioxythiophene (EDOT) substituents by Roncali and co-workers[48,49] or Reynolds and co-workers.[50]

In our experiments, diluted solutions (0.1 mM) of the four thiophene-based monomers containing tetrabutylammonium tetrafluoroborate ($TBABF_4$) in either pure dichloromethane (DCM) or in a mixture of BFEE/DCM (1:4) were first potentiodynamically electropolymerized at platinum disk electrodes. Figure 3 shows the first anodic scan voltammograms for the electropolymerization of the monomers in DCM and BFEE/DCM (1:4).

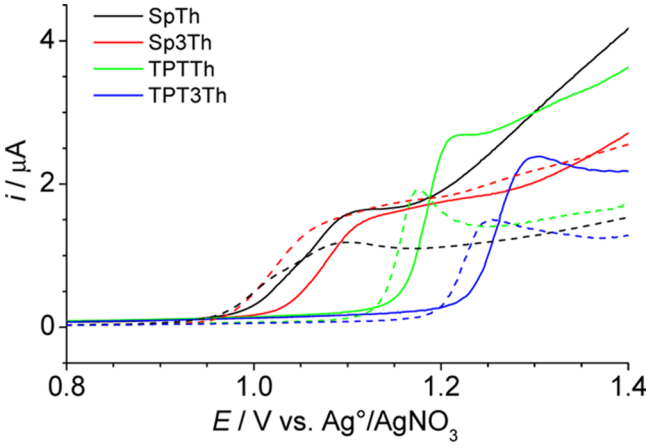


**Figure 3.** First anodic scan voltammograms for 0.1 mM solutions of the monomers and 0.1 M tetrabutylammonium perchlorate in DCM (solid lines) and BFEE/DCM (1:4) (dashed lines) at Pt disk electrodes. The voltammograms were recorded from 0 to 1.4 V with a scan rate of 0.10 V $s^{-1}$.

Two important issues should be mentioned: First, the onsets of the oxidation potential waves for the spirobifluorene-cored monomers are lower than the ones for the tetraphenylmethane-cored monomers (see Table 2). A more extended $\pi$-conjugated

**Table 2. Onset Potential for Electrochemical Polymerization of Thiophene-Based Monomers in Dichloromethane and BFEE/DCM (1:4) Solutions**

| | $E_{onset}$ [V] vs Ag°/$AgNO_3$ | | |
|---|---|---|---|
| monomer | DCM | BFEE/DCM | $\Delta E$ [mV] |
| SpTh | 0.99 | 0.96 | 30 |
| Sp3Th | 1.04 | 0.98 | 60 |
| TPTTh | 1.16 | 1.11 | 50 |
| TPT3Th | 1.23 | 1.20 | 30 |

system in the spirobifluorene-cored monomers hereby causes the decreased oxidation potential. Second, the onset of the oxidation potential waves for all monomers is decreased by addition of BFEE (see Table 2). This phenomenon has been partially explained by a reduced aromaticity of thiophene rings in the presence of a Lewis acid.[34] Hereby, an interaction between the lone pair of the sulfur atom and boron trifluoride leads to this decreased aromaticity, thus causing the decreased oxidation potential.

Cyclic voltammograms for electropolymerization of the monomer solutions in DCM and BFEE/DCM (1:4) at Pt disk electrodes are shown in Figure S4. Repeated scans allowed the consecutive deposition of MPN films on the electrode under observation of progressively increasing anodic and cathodic currents.[51] For SpTh and TPTTh monomers, a quite reversible redox behavior was observed for the deposited MPNs made in the presence of boron trifluoride between 0.6 and 1.1 V. The observed redox response is assigned to the formation of 2,2′-bithiophene bridges (see Scheme 2a). When

**Scheme 2. Idealized Chemical Structures of MPN Films: (a) PSpTh, (b) PSp3Th Prepared in DCM, and (c) PSp3Th Prepared in BFEE/DCM (1:4)**

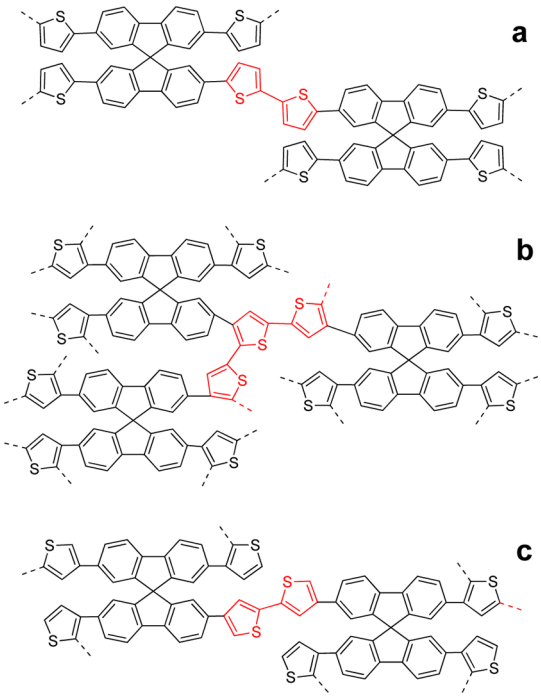


comparing the voltammograms of electropolymerization with and without boron trifluoride for the 3-thienyl-substituted monomers (Sp3Th and TPT3Th), the occurrence of an additional redox peak at lower oxidation potential between 0.2 and 0.6 V is observed for the polymerization of monomer solutions in DCM (without BFEE) that can be ascribed to the formation of branched oligothiophene connections via linking 2- and 5-positions of the 3-thienyl substituents (see Scheme 2b).[42] In contrast, cyclic voltammograms for electropolymerization of the same monomers in the presence of boron trifluoride showed a complete disappearance of these peaks. The observed behavior may indicate that the coupling reaction is limited, in the presence of boron trifluoride, to a dimerization of 3-thienyl substituents as a result of an interaction between Lewis acid and thiophene rings (see Scheme 2c). Cyclic voltammograms for the resulting MPN deposits on Pt disk electrodes in monomer-free DCM solution are shown in Figure S5 at different scan rates from 0.005 to 0.20 V $s^{-1}$. A linear relationship between peak current $i_p$ and scan rate $v$ was observed for all deposits, a characteristic behavior of electroactive materials deposited on an electrode where the current is not diffusion-controlled.[52]

Potentiostatic electrochemical polymerization of 0.5 mM monomer solution in DCM with or without BFEE for 20 min yielded thick, free-standing films which were collected in their dedoped state for the determination of the specific surface area by adsorption/desorption experiments. Around 2 mg of the materials was required for a reliable determination in krypton


DOI: 10.1021/acs.macromol.5b01821
Macromolecules 2015, 48, 6816−6824

sorption experiments at 77 K. Krypton gas has a low saturation pressure of 2.5 Torr at 77 K which is essential for a precise characterization of only small amounts of porous materials.[25] Figure 4 shows the adsorption isotherms in the $P/P_0$ range 0–0.6 using Kr gas at 77 K for all of our thiophene-based MPNs. Similar shapes of the isotherms were observed for all films, regardless the polymerization conditions (with or without BFEE). Alike their chemically synthesized counterparts, at low relative pressure (0–0.1) a quick uptake of sorbate gas ($N_2$ or Kr) was observed which is an indication of permanent microporous materials.[53] Concerning the $S_{BET}$ values determined by applying the BET equation, higher values were obtained for MPN deposits produced in the presence of boron trifluoride (see Table 3). For PSpTh and PTPTTh, $S_{BET}$ values of 815 and 1258 $m^2\ g^{-1}$, respectively, were obtained for deposits produced in the absence of boron trifluoride. These values are much lower compared to their corresponding chemically synthesized counterparts (PSpTh: 1153 $m^2\ g^{-1}$ and PTPTTh: 2020 $m^2\ g^{-1}$). The reduced microporosity could be possibly explained by an incomplete cross-linking of thienyl groups or an overoxidation of the materials at the applied potential of 1.2 V. The addition of BFEE to the polymerization solution led to a significantly increased microporosity with $S_{BET}$ values of 1240 and 2135 $m^2\ g^{-1}$ for PSpTh and PTPTTh, respectively. This means that the addition of boron trifluoride not only decreases the necessary oxidation potential for polymerization but allows for the formation of deposits with increased microporosity. Hereby, $BF_3$-derived anionic species may act as stabilizing counterions during electropolymerization.[54] Moreover, a $S_{BET}$ value of 1576 $m^2\ g^{-1}$ was obtained for PSp3Th films produced in the presence of boron trifluoride. In this case, the obtained specific surface area is higher than the one obtained for the corresponding chemically synthesized polymer (1102 $m^2\ g^{-1}$), possibly related to the preferred formation of bithiophene bridges during the electropolymerization in the presence of boron trifluoride (see Scheme 2). However, this behavior was not observed for PTPT3Th, where the $S_{BET}$ value of 1114 $m^2\ g^{-1}$ for the electrosynthesized film produced in the presence of boron trifluoride was slightly lower than that for the chemically made bulk polymer (1390 $m^2\ g^{-1}$), possibly related to the high oxidation potential of 1.3 V that is required in this case (see Figure 3).

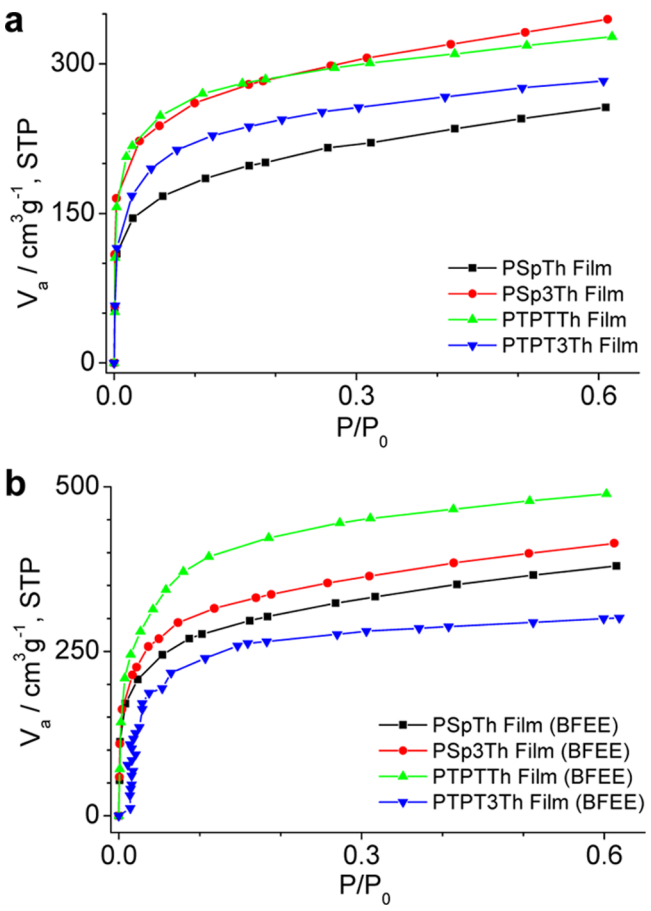


**Figure 4.** Kr gas adsorption isotherms of electropolymerized MPN films prepared in (a) DCM and (b) BFEE/DCM (1:4).

FTIR spectra of monomers, bulk polymers, and MPN films are shown in Figure S6. For the 2-thienyl-based monomers SpTh and TPTTh, peaks at 690 and 699 $cm^{-1}$, respectively, were attributed to out-of-plane CH bending vibrations of monosubstituted thiophene rings.[55] Disappearance of these signals and the occurrence of new bands at 792 and 814 $cm^{-1}$ for PSpTh and 796 and 815 $cm^{-1}$ for PTPTTh reflect the formation of 2,5′-disubstituted bithiophene bridges in the microporous bulk materials or films.[20] Accordingly, the polymers made from 3-thienyl-subtituted monomers showed the disappearance of characteristic peaks for the corresponding monomers at 774 $cm^{-1}$ (Sp3Th) and 773 $cm^{-1}$ (TPT3Th)[56] and the occurrence of a new peak at about 817 $cm^{-1}$ (PSp3Th) and 816 $cm^{-1}$ (PTPT3Th) for 2,3,5-trisubstituted thiophene rings for the bulk polymers and MPN films produced in pure DCM. As expected, MPN films produced in the presence of boron trifluoride exhibited FTIR spectra quite similar to those of the corresponding counterparts made from 2-thienyl-substituted monomers. Here, the presence of two bands at 801 and 818 $cm^{-1}$ for PSp3Th, and 800 and 814 $cm^{-1}$ for PTPT3Th, may indicate the restriction of electropolymerization to the formation of bithiophene linkers. The broad band

**Table 3. Calculated BET Surface Areas by Using Kr Gas Sorption and Optical and Electrochemical Data of Electropolymerized MPN Films, Prepared in DCM and BFEE/DCM (1:4)[a]**

| | $S_{BET}$ [$m^2\ g^{-1}$] | | | | |
|---|---|---|---|---|---|
| MPN films | DCM | BFEE/DCM | $E_g^{opt}$ [b] [eV] | HOMO[elec c] [eV] | LUMO[d] [eV] |
| PSpTh | 815 ± 115 | 1240 ± 84 | −2.72 | −5.61 | −2.89 |
| PSp3Th | 1099 ± 176 | 1576 ± 27 | −2.74 | −5.43 | −2.69 |
| PTPTTh | 1258 ± 52 | 2135 ± 147 | −2.89 | −5.72 | −2.83 |
| PTPT3Th | 927 ± 217 | 1114 ± 197 | −2.73 | −5.65 | −2.92 |

[a]All $S_{BET}$ film measurements were carried four times. [b]Determined from the onset of the absorption band. [c]Taken from the onset of the oxidation wave in monomer-free solution at 0.10 V $s^{-1}$ (see Figure S5). [d]Calculated from the HOMO level by subtracting $E_g^{opt}$.



DOI: 10.1021/acs.macromol.5b01821
Macromolecules 2015, 48, 6816–6824

between 1000 and 1150 $cm^{-1}$ may be related to the presence of some remaining $BF_3$-based (counter)ionic species as impurities of the MPN films.[57] Further characterization experiments of MPN films were carried out with the materials produced in the presence of boron trifluoride. Absorption and PL spectra for the thiophene-based monomers in chloroform and the corresponding MPN thin films produced by potentiodynamic electropolymerization in the presence of boron trifluoride are shown in Figure S7. Red-shifted long wavelength $\pi-\pi^*$ transition bands for the MPN films if compared to the corresponding monomers indicate the presence of more extended $\pi$-conjugated segments in the polymer networks. As the bulk polymers, MPN films on ITO are photoluminescent and might be interesting for applications in chemical sensors.[58,59] Experiments in this direction are underway.

The surface microstructure of our thiophene-based MPN films was studied by tapping mode AFM. A very smooth surface topology was observed for all MPN deposits with average surface roughness ($Rq$) and thickness of 2.5 nm/50.3 nm for PSpTh, 3.6 nm/51.6 nm for PSp3Th, 3.5 nm/44.4 nm for PTPTTh, and 5.3 nm/32.8 nm for PTPT3Th, respectively (see Figure 5 and Table S1). Such morphological properties are

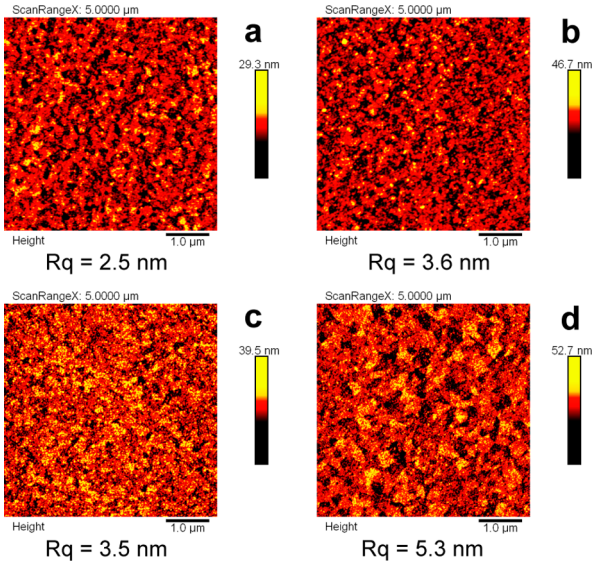


**Figure 5.** Tapping mode AFM images of MPN films on ITO of (a) PSpTh, (b) PSp3Th, (c) PTPTTh, and (d) PTPT3Th. The films were prepared from a 0.1 mM solution of the monomers in BFEE/DCM (1:4) using 0.1 M TBAP as supporting electrolyte. Ten consecutive cyclic voltammograms in the potential range 0−1.2 V (a−c) and 0−1.3 V (d) were applied with a scan rate of 0.1 V $s^{-1}$.

beneficial for a possible application in organic electronics (e.g., OLED, OFET, OPV) where the availability of high quality, uniform, and smooth films is often required.

In a recent publication, we could show a nice correlation between the current response in the electrochemical reduction of a "prototypical" nitroaromatic analyte, 1,3,5-trinitrobenzene (TNB), and the specific surface area of glassy carbon (GC) electrodes modified with carbazole-based MPN coatings.[28] Following this line, we have also produced PTPTTh-modified GC electrodes by applying a potential of 1.2 V until a polymerization charge of 0.2 mC was accumulated, in both DCM and BFEE/DCM. These modified electrodes have been used as working electrode in the reductive electrochemical detection of TNB in aqueous 0.2 M KCl/0.1 M phosphate buffer solution (pH 7.4). Figure 6a shows linear scan voltammograms (LSV) in response to 0.5 mM TNB, after background correction, for non- and PTPTTh-modified GC electrodes. Three cathodic peaks are observed for reduction of the three nitro groups of TNB to hydroxylamine groups.[60]

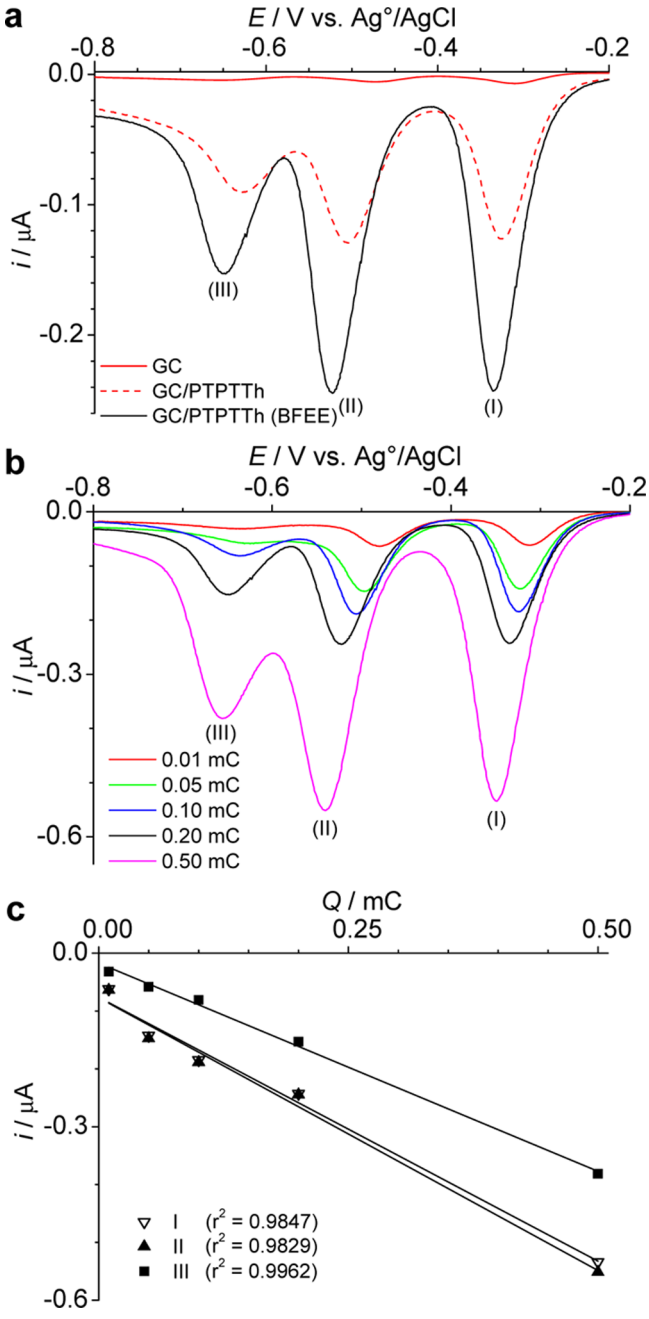


**Figure 6.** Linear scan voltammograms (LSV) for the reduction of 0.5 $\mu$M TNB in aqueous 0.2 M KCl and 0.1 M PBS solution (a) at nonmodified and PTPTTh-modified GC electrodes prepared in DCM and BFEE/DCM (1:4) solutions for an accumulated charge during electropolymerization of 0.20 mC, (b) PTPTTh-modified GC electrodes prepared in BFEE/DCM (1:4) solution for an accumulated charges during electropolymerization from 0.01 to 0.50 mC, and (c) plot of peak current versus accumulated charge during electropolymerization under formation of PTPTTh-modified GC electrodes in BFEE/DCM (1:4) solution. LSVs were obtained with a scan rate of 0.01 V $s^{-1}$.



DOI: 10.1021/acs.macromol.5b01821
*Macromolecules* 2015, 48, 6816−6824

Peaks at about −0.31 V (I), −0.47 V (II), and −0.65 V (III) were observed in accordance with literature results.[61] A much increased current response was observed for PTPTTh-modified GC electrodes if compared to the bare, nonmodified GC electrode. This phenomenon is most probably driven by strong interactions at the surface of the microporous materials with their high specific surface area. Such behavior has been related to the formation of charge-transfer complexes (Jack−Meisenheimer complexes) between electron-rich (e.g., amines, carbazoles, and thiophenes) and electron-poor structural units (e.g., nitroaromatic analytes) by decreasing the interfacial charge-transfer resistance.[62] The influence of the surface area is clearly demonstrated by comparing the TNB reduction response of two PTPTTh-modified GC electrodes, whereby the electrode coating are made with and without BFEE as additive. The charge ratio in the reduction of TNB of 1.5 corresponds nicely to the $S_{BET}$ ratio of 1.7 for the two materials (see Table 3). Linear scan voltammograms of the reduction of 0.5 mM aqueous TNB solution depicted in Figure 6b for different thicknesses of the PTPTTh deposits on GC electrodes (produced in the presence of boron trifluoride by varying the accumulated charge during polymerization). Similar three reduction peaks were observed with slight negative shifts of the potential for increasing thickness. A plot of reduction current response versus the accumulated charge during fabrication of the PTPTTh films (as an indirect measure of the film thickness) demonstrates a linear relationship and support our assumption of a strong interaction of the nitroaromatic analytes with the surface of the microporous deposits.

Finally, in an orienting experiment the detection range in the electrochemical reduction of TNB in aqueous solution was tested for different TNB concentrations (0.5−3.0 $\mu$M) at PTPTTh-modified GC electrodes (see Figure S8). For a nonmodified GC electrode, a linear relation between current response and concentration is observed in the studied concentration range, indicating that the process is diffusion-controlled. For the PTPTTh-modified GC electrodes, the current response shows a turning point saturation for a concentration of ca. 1.5 $\mu$M TNB. This phenomenon may be related to an adsorption-controlled process in the concentration range between 0 and 1.5 $\mu$M TNB, for the low scan rate of 0.01 V $s^{-1}$ applied. A similar behavior was reported by us for carbazole-based MPN films.[28]

## CONCLUSIONS

To sum up, a series of tetrafunctional thiophene-based monomers were chemically and electrochemically polymerized, resulting in microporous polymer networks with high specific surface areas of up to 2135 $m^2$ $g^{-1}$ for thin films and 2020 $m^2$ $g^{-1}$ for powdery bulk materials. All materials showed a good thermal stability and were PL-active. Electrochemical polymerization in dichloromethane (DCM)/boron trifluoride diethyl etherate (BFEE) mixtures generally produced MPN films with higher surface area and a more defined electrochemical behavior if compared to ones made in pure DCM. Different coupling patterns have been observed for 3-thienyl-substituted monomers in the presence or absence of boron trifluoride as additive: In the presence of BFEE the preferred formation of bithiophene bridges was observed, thus enhancing the microporosity of the materials. The aqueous electrochemical reduction of TNB at nonmodified and PTPTTh-modified GC electrodes showed a much increased cathodic current response for the modified electrodes, most probably driven by interactions of electron-poor nitroaromatic analyte molecules and the electron-rich thiophene-based MPN films with their high surface area. Favorably, our MPN films were characterized by a pretty smooth morphology with a low average surface roughness <5.3 nm, thus encouraging upcoming experiments toward an application in organic electronics devices.

## ASSOCIATED CONTENT

### Supporting Information

The Supporting Information is available free of charge on the ACS Publications website at DOI: 10.1021/acs.macromol.5b01821.

Materials and methods; TGA plots and gas sorption isotherms for the bulk polymers; cyclic voltammograms for the electropolymerization of the monomers on Pt disk electrodes; FTIR, UV−vis, and PL spectra of the materials; AFM images of MPN films, including surface roughness and thickness data; electrochemical characterization data for the aqueous detection of 1,3,5-trinitrobenzene (PDF)

## AUTHOR INFORMATION

### Corresponding Author

*E-mail: scherf@uni-wuppertal.de (U.S.).

### Funding

Research Grants for Doctoral Candidates and Young Academics and Scientists, A/12/74361, German Academic Exchange Service (DAAD).

### Notes

The authors declare no competing financial interest.

## ACKNOWLEDGMENTS

We thank Prof. Thomas Riedl for the access to the profilometer and Silvia Adamczyk for the AFM measurements. A. Palma-Cando thanks the German Academic Exchange Service (DAAD) for granting him a Ph.D. scholarship.

## REFERENCES

(1) Chen, Q.; Liu, D.-P.; Luo, M.; Feng, L.-J.; Zhao, Y.-C.; Han, B.-H. Nitrogen-Containing Microporous Conjugated Polymers via Carbazole-Based Oxidative Coupling Polymerization: Preparation, Porosity, and Gas Uptake. *Small* **2014**, *10*, 308−315.

(2) Fischer, S.; Schimanowitz, A.; Dawson, R.; Senkovska, I.; Kaskel, S.; Thomas, A. Cationic Microporous Polymer Networks by Polymerisation of Weakly Coordinating Cations With $CO_2$-Storage Ability. *J. Mater. Chem. A* **2014**, *2*, 11825−11829.

(3) Chen, Q.; Liu, D.-P.; Zhu, J.-H.; Han, B.-H. Mesoporous Conjugated Polycarbazole with High Porosity via Structure Tuning. *Macromolecules* **2014**, *47*, 5926−5931.

(4) Chen, Q.; Luo, M.; Hammershøj, P.; Zhou, D.; Han, Y.; Laursen, B. W.; Yan, C.-G.; Han, B.-H. Microporous Polycarbazole with High Specific Surface Area for Gas Storage and Separation. *J. Am. Chem. Soc.* **2012**, *134*, 6084−6087.

(5) Sekizkardes, A. K.; Altarawneh, S.; Kahveci, Z.; İslamoğlu, T.; El-Kaderi, H. M. Highly Selective $CO_2$ Capture by Triazine-Based Benzimidazole-Linked Polymers. *Macromolecules* **2014**, *47*, 8328−8334.

(6) Sekizkardes, A. K.; Culp, J. T.; Islamoglu, T.; Marti, A.; Hopkinson, D.; Myers, C.; El-Kaderi, H. M.; Nulwala, H. B. An Ultra-Microporous Organic Polymer for High Performance Carbon Dioxide Capture and Separation. *Chem. Commun.* **2015**, *51*, 13393−13396.

(7) Zhang, Y.; A, S.; Zou, Y.; Luo, X.; Li, Z.; Xia, H.; Liu, X.; Mu, Y. Gas Uptake, Molecular Sensing and Organocatalytic Performances of a



DOI: 10.1021/acs.macromol.5b01821
*Macromolecules* 2015, 48, 6816−6824

Multifunctional Carbazole-Based Conjugated Microporous Polymer. *J. Mater. Chem. A* **2014**, *2*, 13422−13430.
(8) Zhao, Q.; Zhang, P.; Antonietti, M.; Yuan, J. Poly(ionic liquid) Complex with Spontaneous Micro-/Mesoporosity: Template-Free Synthesis and Application as Catalyst Support. *J. Am. Chem. Soc.* **2012**, *134*, 11852−11855.
(9) Rose, M. Nanoporous Polymers: Bridging the Gap between Molecular and Solid Catalysts? *ChemCatChem* **2014**, *6*, 1166−1182.
(10) Bleschke, C.; Schmidt, J.; Kundu, D. S.; Blechert, S.; Thomas, A. A Chiral Microporous Polymer Network as Asymmetric Heterogeneous Organocatalyst. *Adv. Synth. Catal.* **2011**, *353*, 3101−3106.
(11) Kundu, D. S.; Schmidt, J.; Bleschke, C.; Thomas, A.; Blechert, S. A Microporous Binol-Derived Phosphoric Acid. *Angew. Chem., Int. Ed.* **2012**, *51*, 5456−5459.
(12) Akiyama, T.; Matsushita, M.; Kakutani, K.; Yamada, S.; Takechi, K.; Shiga, T.; Motohiro, T.; Nakayama, H.; Kohama, K. Solid-State Solar Cells Consisting of Polythiophene-Porphyrin Composite Films. *Jpn. J. Appl. Phys.* **2005**, *44*, 2799−2802.
(13) Roncali, J.; Leriche, P.; Cravino, A. From One- to Three-Dimensional Organic Semiconductors: In Search of the Organic Silicon? *Adv. Mater.* **2007**, *19*, 2045−2060.
(14) Xu, Y.; Jin, S.; Xu, H.; Nagai, A.; Jiang, D. Conjugated Microporous Polymers: Design, Synthesis and Application. *Chem. Soc. Rev.* **2013**, *42*, 8012−8031.
(15) Preis, E.; Dong, W.; Brunklaus, G.; Scherf, U. Microporous, Tetraarylethylene-Based Polymer Networks Generated in a Reductive Polyolefination Process. *J. Mater. Chem. C* **2015**, *3*, 1582−1587.
(16) Zhang, K.; Kopetzki, D.; Seeberger, P. H.; Antonietti, M.; Vilela, F. Surface Area Control and Photocatalytic Activity of Conjugated Microporous Poly(benzothiadiazole) Networks. *Angew. Chem., Int. Ed.* **2013**, *52*, 1432−1436.
(17) Liu, X.; Xu, Y.; Jiang, D. Conjugated Microporous Polymers as Molecular Sensing Devices: Microporous Architecture Enables Rapid Response and Enhances Sensitivity in Fluorescence-On and Fluorescence-Off Sensing. *J. Am. Chem. Soc.* **2012**, *134*, 8738−8741.
(18) Yuan, D.; Lu, W.; Zhao, D.; Zhou, H.-C. Highly Stable Porous Polymer Networks with Exceptionally High Gas-Uptake Capacities. *Adv. Mater.* **2011**, *23*, 3723−3725.
(19) Dawson, R.; Stockel, E.; Holst, J. R.; Adams, D. J.; Cooper, A. I. Microporous Organic Polymers for Carbon Dioxide Capture. *Energy Environ. Sci.* **2011**, *4*, 4239−4245.
(20) Yuan, S.; Kirklin, S.; Dorney, B.; Liu, D.-J.; Yu, L. Nanoporous Polymers Containing Stereocontorted Cores for Hydrogen Storage. *Macromolecules* **2009**, *42*, 1554−1559.
(21) Schmidt, J.; Weber, J.; Epping, J. D.; Antonietti, M.; Thomas, A. Microporous Conjugated Poly(thienylene arylene) Networks. *Adv. Mater.* **2009**, *21*, 702−705.
(22) Gu, C.; Chen, Y.; Zhang, Z.; Xue, S.; Sun, S.; Zhang, K.; Zhong, C.; Zhang, H.; Pan, Y.; Lv, Y.; Yang, Y.; Li, F.; Zhang, S.; Huang, F.; Ma, Y. Electrochemical Route to Fabricate Film-Like Conjugated Microporous Polymers and Application for Organic Electronics. *Adv. Mater.* **2013**, *25*, 3443−3448.
(23) Gu, C.; Chen, Y.; Zhang, Z.; Xue, S.; Sun, S.; Zhong, C.; Zhang, H.; Lv, Y.; Li, F.; Huang, F.; Ma, Y. Achieving High Efficiency of PTB7-Based Polymer Solar Cells via Integrated Optimization of Both Anode and Cathode Interlayers. *Adv. Energy Mater.* **2014**, *4*, 1301771−1301775.
(24) Zhang, H.; Zhang, Y.; Gu, C.; Ma, Y. Electropolymerized Conjugated Microporous Poly(zinc-porphyrin) Films as Potential Electrode Materials in Supercapacitors. *Adv. Energy Mater.* **2015**, *5*, 1402175−1402180.
(25) Gu, C.; Huang, N.; Gao, J.; Xu, F.; Xu, Y.; Jiang, D. Controlled Synthesis of Conjugated Microporous Polymer Films: Versatile Platforms for Highly Sensitive and Label-Free Chemo- and Biosensing. *Angew. Chem., Int. Ed.* **2014**, *53*, 4850−4855.
(26) Gu, C.; Huang, N.; Wu, Y.; Xu, H.; Jiang, D. Design of Highly Photofunctional Porous Polymer Films with Controlled Thickness and Prominent Microporosity. *Angew. Chem., Int. Ed.* **2015**, DOI: 10.1002/anie.201504786.
(27) Gu, C.; Huang, N.; Xu, F.; Gao, J.; Jiang, D. Cascade Exciton-Pumping Engines with Manipulated Speed and Efficiency in Light-Harvesting Porous π-Network Films. *Sci. Rep.* **2015**, *5*, 8867−8874.
(28) Palma-Cando, A.; Scherf, U. Electrogenerated Thin Films of Microporous Polymer Networks with Remarkably Increased Electrochemical Response to Nitroaromatic Analytes. *ACS Appl. Mater. Interfaces* **2015**, *7*, 11127−11133.
(29) Roncali, J.; Thobie-Gautier, C.; Brisset, H.; Favart, J.-F.; Guy, A. Electro-Oxidation of Tetra(terthienyl)silanes: Towards 3D Electroactive π-Conjugated Systems. *J. Electroanal. Chem.* **1995**, *381*, 257−260.
(30) John, H.; Bauer, R.; Espindola, P.; Sonar, P.; Heinze, J.; Müllen, K. 3D-Hybrid Networks with Controllable Electrical Conductivity from the Electrochemical Deposition of Terthiophene-Functionalized Polyphenylene Dendrimers. *Angew. Chem., Int. Ed.* **2005**, *44*, 2447−2451.
(31) Bildirir, H.; Osken, I.; Ozturk, T.; Thomas, A. Reversible Doping of a Dithienothiophene-Based Conjugated Microporous Polymer. *Chem.—Eur. J.* **2015**, DOI: 10.1002/chem.201582661.
(32) Shi, G.; Jin, S.; Xue, G.; Li, C. A Conducting Polymer Film Stronger Than Aluminum. *Science* **1995**, *267*, 994−996.
(33) Jin, S.; Xue, G. Interaction between Thiophene and Solvated Lewis Acids and the Low-Potential Electrochemical Deposition of a Highly Anisotropic Conducting Polythiophene Film. *Macromolecules* **1997**, *30*, 5753−5757.
(34) Shi, G.; Li, C.; Liang, Y. High-Strength Conducting Polymers Prepared by Electrochemical Polymerization in Boron Trifluoride Diethyl Etherate Solution. *Adv. Mater.* **1999**, *11*, 1145−1146.
(35) Wang, X.; Yue, R.; Lu, B.; Wei, Z.; Xu, J. Synthesis and Electrochemical Polymerization of 9,9-bis(carbazolylalkyl)fluorene and Characterization of its Conducting Polymer Film with High Tensile Strength. *J. Mater. Sci.* **2010**, *45*, 1963−1971.
(36) Jiang, J.-X.; Su, F.; Trewin, A.; Wood, C. D.; Campbell, N. L.; Niu, H.; Dickinson, C.; Ganin, A. Y.; Rosseinsky, M. J.; Khimyak, Y. Z.; Cooper, A. I. Conjugated Microporous Poly(aryleneethynylene) Networks. *Angew. Chem.* **2007**, *119*, 8728−8732.
(37) Ben, T.; Ren, H.; Ma, S.; Cao, D.; Lan, J.; Jing, X.; Wang, W.; Xu, J.; Deng, F.; Simmons, J. M.; Qiu, S.; Zhu, G. Targeted Synthesis of a Porous Aromatic Framework with High Stability and Exceptionally High Surface Area. *Angew. Chem.* **2009**, *121*, 9621−9624.
(38) Preis, E.; Widling, C.; Scherf, U.; Patil, S.; Brunklaus, G.; Schmidt, J.; Thomas, A. Aromatic, Microporous Polymer Networks with High Surface Area Generated in Friedel-Crafts-Type Polycondensations. *Polym. Chem.* **2011**, *2*, 2186−2189.
(39) Sing, K. S. W. Reporting Physisorption Data for Gas/Solid Systems with Special Reference to the Determination of Surface Area and Porosity (Recommendations 1984). *Pure Appl. Chem.* **1985**, *57*, 603−619.
(40) Qiao, S.; Du, Z.; Yang, R. Design and Synthesis of Novel Carbazole-Spacer-Carbazole Type Conjugated Microporous Networks for Gas Storage and Separation. *J. Mater. Chem. A* **2014**, *2*, 1877−1885.
(41) Yan, Q.; Lin, Y.; Kong, C.; Chen, L. Remarkable $CO_2$/CH4 Selectivity and $CO_2$ Adsorption Capacity Exhibited by Polyamine-Decorated Metal-Organic Framework Adsorbents. *Chem. Commun.* **2013**, *49*, 6873−6875.
(42) Heinze, J.; Frontana-Uribe, B. A.; Ludwigs, S. Electrochemistry of Conducting Polymers-Persistent Models and New Concepts. *Chem. Rev.* **2010**, *110*, 4724−4771.
(43) Palma-Cando, A. U.; Frontana-Uribe, B. A.; Maldonado, J. L.; Hernández, M. R. Control of Thickness of PEDOT Electrodeposits on Glass/ITO Electrodes from Organic Solutions and its Use as Anode in Organic Solar Cells. *Procedia Chem.* **2014**, *12*, 92−99.
(44) Argun, A. A.; Aubert, P.-H.; Thompson, B. C.; Schwendeman, I.; Gaupp, C. L.; Hwang, J.; Pinto, N. J.; Tanner, D. B.; MacDiarmid, A. G.; Reynolds, J. R. Multicolored Electrochromism in Polymers: Structures and Devices. *Chem. Mater.* **2004**, *16*, 4401−4412.
(45) Zotti, G.; Zecchin, S.; Schiavon, G.; Louwet, F.; Groenendaal, L.; Crispin, X.; Osikowicz, W.; Salaneck, W.; Fahlman, M. Electro-


DOI: 10.1021/acs.macromol.5b01821
*Macromolecules* 2015, 48, 6816−6824

chemical and XPS Studies toward the Role of Monomeric and Polymeric Sulfonate Counterions in the Synthesis, Composition, and Properties of Poly(3,4-ethylenedioxythiophene). *Macromolecules* **2003**, *36*, 3337−3344.
(46) Ma, W.; Yang, C.; Gong, X.; Lee, K.; Heeger, A. J. Thermally Stable, Efficient Polymer Solar Cells with Nanoscale Control of the Interpenetrating Network Morphology. *Adv. Funct. Mater.* **2005**, *15*, 1617−1622.
(47) Zhang, H.; Azimi, H.; Hou, Y.; Ameri, T.; Przybilla, T.; Spiecker, E.; Kraft, M.; Scherf, U.; Brabec, C. J. Improved High-Efficiency Perovskite Planar Heterojunction Solar Cells via Incorporation of a Polyelectrolyte Interlayer. *Chem. Mater.* **2014**, *26*, 5190−5193.
(48) Piron, F.; Leriche, P.; Mabon, G.; Grosu, I.; Roncali, J. Electropolymerization of Three-Dimensional $\pi$-Conjugated System Based on 3,4-Ethylenedioxythiophene (EDOT). *Electrochem. Commun.* **2008**, *10*, 1427−1430.
(49) Piron, F.; Leriche, P.; Grosu, I.; Roncali, J. Electropolymerizable 3D$\pi$-Conjugated Architectures with Ethylenedioxythiophene (EDOT) End-Groups as Precursors of Electroactive Conjugated Networks. *J. Mater. Chem.* **2010**, *20*, 10260−10268.
(50) Reeves, B. D.; Thompson, B. C.; Abboud, K. A.; Smart, B. E.; Reynolds, J. R. Dual Cathodically and Anodically Coloring Electrochromic Polymer Based on a Spiro Bipropylenedioxythiophene [(Poly(spiroBiProDOT)]. *Adv. Mater.* **2002**, *14*, 717−719.
(51) Kumar, A.; Welsh, D. M.; Morvant, M. C.; Piroux, F.; Abboud, K. A.; Reynolds, J. R. Conducting Poly(3,4-alkylenedioxythiophene) Derivatives as Fast Electrochromics with High-Contrast Ratios. *Chem. Mater.* **1998**, *10*, 896−902.
(52) Wei, Y.; Chan, C. C.; Tian, J.; Jang, G. W.; Hsueh, K. F. Electrochemical Polymerization of Thiophenes in the Presence of Bithiophene or Terthiophene: Kinetics and Mechanism of the Polymerization. *Chem. Mater.* **1991**, *3*, 888−897.
(53) Jiang, M.-Y.; Wang, Q.; Chen, Q.; Hu, X.-M.; Ren, X.-L.; Li, Z.-H.; Han, B.-H. Preparation and Gas Uptake of Microporous Organic Polymers Based on Binaphthalene-Containing Spirocyclic Tetraether. *Polymer* **2013**, *54*, 2952−2957.
(54) Alkan, S.; Cutler, C. A.; Reynolds, J. R. High-Quality Electrochromic Polythiophenes via BF3·Et2O Electropolymerization. *Adv. Funct. Mater.* **2003**, *13*, 331−336.
(55) Wang, B.; Zhao, J.; Cui, C.; Liu, J.; He, Q. Electrosynthesis and Characterization of an Electrochromic Material from Poly(1,4-bis(3-methylthiophen-2-yl)benzene) and its Application in Electrochromic Device. *Sol. Energy Mater. Sol. Cells* **2012**, *98*, 161−167.
(56) Rosatzin, H. I. Infrared Study of Substituted Thiophenes in the Low-Frequency Region. *Spectrochim. Acta* **1963**, *19*, 1107−1118.
(57) Latonen, R.-M.; Kvarnström, C.; Ivaska, A. In Situ UV−vis and FTIR Attenuated Total Reflectance Studies on the Electrochemically Synthesized Copolymer from Biphenyl and 3-Octylthiophene. *J. Electroanal. Chem.* **2001**, *512*, 36−48.
(58) Dong, W.; Fei, T.; Palma-Cando, A.; Scherf, U. Aggregation Induced Emission and Amplified Explosive Detection of Tetraphenylethylene-Substituted Polycarbazoles. *Polym. Chem.* **2014**, *5*, 4048−4053.
(59) Ma, H.; Yao, L.; Li, P.; Ablikim, O.; Cheng, Y.; Zhang, M. Highly Sensitive and Selective Fluorometric/Electrochemical Dual-Channel Sensors for TNT and DNT Explosives. *Chem. - Eur. J.* **2014**, *20*, 11655−11658.
(60) Laviron, E.; Meunier-Prest, R.; Vallat, A.; Roullier, L.; Lacasse, R. The Reduction Mechanism of Aromatic Nitro Compounds in Aqueous Medium: Part II. The Reduction of 4-nitropyridine Between H0 = − 6 and pH 9.6. *J. Electroanal. Chem.* **1992**, *341*, 227−255.
(61) Zhang, H.-X.; Cao, A.-M.; Hu, J.-S.; Wan, L.-J.; Lee, S.-T. Electrochemical Sensor for Detecting Ultratrace Nitroaromatic Compounds Using Mesoporous $SiO_2$-Modified Electrode. *Anal. Chem.* **2006**, *78*, 1967−1971.
(62) Shamsipur, M.; Tabrizi, M. A.; Mahkam, M.; Aboudi, J. A High Sensitive TNT Sensor Based on Electrochemically Reduced Graphene Oxide-Poly(amidoamine) Modified Electrode. *Electroanalysis* **2015**, *27*, 1466−1472.


DOI: 10.1021/acs.macromol.5b01821
*Macromolecules* 2015, 48, 6816−6824